

Electronic Structure Analysis and Electron Detachment Energies of Polynitrogen Pentagonal Aromatic Anions

Junia Melin,[†] Manoj K. Mishra,[‡] and J. V. Ortiz^{*,†}

Department of Chemistry, Kansas State University, Manhattan, Kansas 66506-3701,

Department of Chemistry and Biochemistry, Auburn University, Auburn, Alabama 36849-5312, and

Department of Chemistry, Indian Institute of Technology, Bombay, Powai, Mumbai 400 076, India

Received: May 27, 2006; In Final Form: September 1, 2006

Various decouplings of the electron propagator have been employed to provide theoretical comparison to experimental electron detachment energies for the pyrrolide, imidazolide, and pyrazolide anions. Predictions for isoelectronic anions in which CH groups are replaced by N atoms also are reported. The ab initio electron propagator results agree closely with experimental values, and the associated Dyson orbitals provide a detailed catalog of bonding changes as the number and positions of N atoms vary within the set of pentagonal aromatic anions.

I. Introduction

The homonuclear polynitrogen compound pentazole, N_5^- , has been a source of much theoretical and experimental interest for its promise as a high energy-density material (HEDM) with environmentally benign decomposition products.^{1–8} A systematic investigation of the photoelectron spectra of some of its isoelectronic analogues, the pyrrolide, imidazolide, and pyrazolide anions, has been reported recently.^{9–11} Imidazole appears in the side chain of the amino acid histidine with important links to diverse biological activities, and the other isoelectronic pentagonal variants containing two, three, or four nitrogens in differing arrangements have a multiplicity of similarly important connections to several areas of biological and pharmaceutical chemistry.⁸

Many different routes to the synthesis of N_5^- have been attempted,^{5,6} and this anion has been studied with B3LYP^{3,5} and CASSCF² calculations. Hydrogen pentazole has been examined with the MBPT(2) and CCSD methods.¹ B3LYP^{9–11} calculations have been performed on the pyrrolide and imidazolide anions. The remaining isoelectronic, pentagonal, aromatic, heterocyclic anions have been investigated using B3LYP⁴ and MNDO.⁸

The electron propagator⁹ has emerged as a powerful tool for direct and correlated calculation of ionization energies and electron affinities. Dyson orbitals, which can be used to decipher the energy level changes attending electron detachment and attachment processes,^{10,11} also have been used extensively for treatment of ionization energies and electron affinities for a large variety of systems.¹² The availability of well-resolved, experimental, photoelectron spectra for pyrrolide, imidazolide, and pyrazolide anions has prompted us to attempt a systematic investigation of electron detachments from pentazole and several isoelectronic anions. It is our purpose in this paper to apply various decouplings of the electron propagator, using sufficiently large basis sets to provide dependable results, which can be compared with photoelectron data that are available

already. We also predict electron detachment energies for related anions whose photoelectron spectra have not been reported so far. An investigation of the changes in electron detachment energies as a function of the number and position of nitrogen atoms in these pentagonal, aromatic anions and a correlation of these changes with orbital attributes also are attempted in this work.

The electron propagator method is well established,¹⁶ and only a skeletal outline with some computational details is offered in the next section. Results are discussed in section III, and a brief summary of major results concludes this paper.

II. Methods

Electron propagator calculations¹⁶ for vertical electron attachment and detachment energies are based on the Dyson equation. A convenient form of this equation reads

$$[\hat{f} + \hat{\Sigma}(\epsilon_i)]\phi_i^{\text{Dyson}}(x) = \epsilon_i\phi_i^{\text{Dyson}}(x) \quad (1)$$

Here, \hat{f} is the one-electron Fock operator, and $\hat{\Sigma}(\epsilon)$ is the energy-dependent, nonlocal self-energy operator which accounts for correlation and orbital relaxation effects.

The eigenfunctions of eq 1 are the Dyson orbitals, ϕ_i^{Dyson} , and for electron detachment processes they are defined as

$$\phi_i^{\text{IP,Dyson}}(x_N) = \sqrt{N} \int \Psi_N(x_1, \dots, x_N) \Psi_{i,N-1}^*(x_1, \dots, x_{N-1}) dx_1 dx_2 dx_3 \dots dx_{N-1} \quad (2)$$

where $\Psi_N(x_1, \dots, x_N)$ is the wave function for the N -electron initial state, and $\Psi_{i,N-1}(x_1, \dots, x_{N-1})$ is the wave function for the i th final state with $N - 1$ electrons. In this expression, x_j represents the space-spin coordinates of electron j .

Once the Dyson equation is solved self-consistently, orbital energy values, ϵ_i , are obtained. These values correspond to electron binding energies of the molecular system and therefore can be directly compared with photoelectron spectra.

Perturbative arguments can be used to neglect off-diagonal matrix elements of the self-energy operator in the Hartree–Fock (HF) basis, which leads to a quasi-particle expression for

* Corresponding author e-mail: ortiz@auburn.edu.

[†] Kansas State University and Auburn University.

[‡] Kansas State University and Indian Institute of Technology.

TABLE 1: Pyrrolide and Pyrrolyl Geometrical Parameters^a

	pyrrolide (¹ A ₁)				pyrrolyl (² A ₂)			
	MP2	QCISD	CCSD	DFT ^b	MP2	QCISD	CCSD	DFT ^b
d(N-C ₁)	1.3695	1.366	1.3653	1.3625	1.336	1.3484	1.347	1.3441
d(C ₁ -C ₂)	1.4098	1.4066	1.4065	1.4035	1.4504	1.4684	1.468	1.4598
d(C ₂ -C ₃)	1.4214	1.4255	1.4247	1.4195	1.377	1.3637	1.3633	1.361
d(C ₁ -H ₅)	1.0885	1.0891	1.0889	1.0865	1.085	1.0854	1.0853	1.0834
d(C ₂ -H ₆)	1.0871	1.0875	1.0872	1.0847	1.0813	1.0827	1.0825	1.0798
A(N-C ₁ -C ₂)	112.27	112.35	112.34	112.06	113.41	112.41	112.44	112.38
A(C ₁ -C ₂ -C ₃)	105.37	105.24	105.24	105.38	104.56	105.23	105.2	105.25
A(C ₄ -N-C ₁)	104.72	104.82	104.84	105.13	104.05	104.71	104.72	104.75
A(N-C ₁ -H ₅)	120.37	120.37	120.39	120.54	120.73	120.96	120.97	120.99
A(C ₁ -C ₂ -H ₆)	127.13	127.16	127.15	127.2	126.72	126.17	126.18	126.26

^a Distances in Å and angles in degree. All structures are planar. ^b Values from ref 10.

the electron binding energies, $E = e_i^{\text{HF}} + \sum_{ii}(E)$. The electron propagator calculations utilized in this study are based on this class of approximation, namely, diagonal second and third order, P3 and OVGf.^{16a,b}

The norm of the Dyson orbital, p_i , is known as the pole strength. Its definition reads

$$p_i = \int |\phi_i^{\text{Dyson}}(x)|^2 dx \quad (3)$$

Thus, the Dyson orbital, within the diagonal approximation, is given by the square root of the pole strength times a canonical HF orbital

$$\phi_i^{\text{Dyson}}(x) = \sqrt{p_i} \psi_i^{\text{HF}}(x) \quad (4)$$

The pole strength is like a normalizing factor, which takes values between zero and unity. It therefore is an index of the validity of the diagonal approximations. If the ionization process is well described by a Koopmans frozen-orbital picture, pole strengths are very close to 1.0. On the other hand, pole strengths that are less than 0.8 indicate that electron correlation has qualitative importance for the ionization.

Geometry optimizations and frequency calculations for all systems under study were performed with Gaussian03.¹³ The P3+ method,¹⁸ recently developed in our group, required a modified version of the standard electron propagator code.

III. Results and Discussion

Pyrrolide. In a recent report of Lineberger and collaborators,⁹ the 3.408 eV photoelectron spectrum of the pyrrolide anion has been analyzed. This spectrum shows a main peak at 2.145 ± 0.01 eV followed by three minor features that were assigned to totally symmetric vibrational modes of the pyrrolyl radical.

We have performed geometry optimizations at several levels of theory for the pyrrolide anion as well as for the pyrrolyl radical in its ²A₂ ground state. Table 1 summarizes these results. We found that the pyrrolide and pyrrolyl geometries are quite stable with respect to correlation treatments. Similar structures are obtained with the MP2, QCISD, and CCSD methods, and they are in good agreement with previous DFT⁹ calculations. However, the results do not seem to be stable with respect to the basis set. The first attempt at optimizing the pyrrolide anion using the 6-311++G(d,p) standard basis set has found minima at the QCISD and CCSD levels of theory, but an imaginary frequency appears with MP2. After augmenting the basis set by including *f*-type polarization functions, this imaginary frequency disappears and a minimum is found. Whereas MP2/6-311++(2df,2p) optimizations are less time-consuming than QCISD or CCSD calculations, they produce similar geometries.

TABLE 2: Adiabatic Electron Affinities of Pyrrolyl and Geometrical Relaxation Energies of Pyrrolyl with Respect to Pyrrolide Geometries (eV)

	6-311++G(d,p)			
	MP2 6-311++G(2df,2p)	QCISD	CCSD	B3LYP
adiabatic EA	2.54	1.78	1.79	2.12 ^a
relaxation energy	0.18	0.22	0.22	

^a Reference 9.

Therefore, subsequent optimizations will be performed with the MP2 method and the latter basis set.

Total energies and adiabatic electron affinities of the pyrrolyl radical calculated with MP2, QCISD, and CCSD are listed in Table 2. Zero-point corrections are not included. Whereas the B3LYP result of ref 9 is in excellent agreement with the experimentally determined value of the same article, larger discrepancies obtain for the other methods. Because larger basis sets generally lead to increased electron binding energies, the QCISD and CCSD methods may be capable of producing lower errors with respect to experiment.

Vertical electron detachment energies (VEDEs) for the anionic systems were calculated using electron propagator methods and the 6-311++(2df,2p) basis set. Table 3 shows the VEDE results and the corresponding orbital pictures. Pole strengths are larger than 0.85 in all cases, with the lone exception of the second ²B₁ state, which presents a pole value near 0.8. Such results are typical for the most highly bound π orbital. The OVGf, P3, and P3+ methods produce VEDEs that are larger than the experimental adiabatic electron affinity by 0.08–0.25 eV. The latter figures are in good agreement with geometry relaxation energies of Table 2 and confirm the predictive capabilities of these three electron propagator approximations.

Diazolides. An experimental photoelectron spectrum has been reported for the imidazolide anion recently.¹⁰ As can be seen from Table 4, the VEDE results calculated from the OVGf, P3, and P3+ approximations lie 0.1–0.3 eV above the experimental value for the adiabatic electron affinity. For the highest ²A₁ and ²B₁ final states, correlated decouplings reverse the order predicted by KT results. The correlated predictions offer a more authoritative guide for assigning the higher electron detachment energies of the imidazolide anion, which have not been determined yet by experiment.

As may be seen from the orbital plots, the electron binding energies are directly related to the extent of localization of the orbital density on the nitrogen atoms in the imidazole ring. The Dyson orbital for the lowest electron detachment energy has little participation from the two nitrogen atoms and is a carbon-centered, π orbital. (Similar conclusions on diazolidate orbitals were reached in refs 10 and 11.) A predominantly nitrogen-

TABLE 3: Vertical Electron Detachment Energies (eV) and Orbitals for Pyrrolide^a

	² A ₂ ⁺	² B ₁	² A ₁	² B ₁ [*]	² A ₁	² B ₂	² B ₂	² A ₁
KT	-2.16	-3.09	-5.71	-8.65	-8.87	-9.08	-9.35	-13.14
2Ord	-1.93	-2.39	-2.88	-6.29	-6.60	-6.91	-7.03	-10.19
3Ord	-2.35	-3.10	-5.10	-7.64	-8.04	-8.22	-8.69	-11.92
OVSF	-2.23	-2.75	-4.19	-7.10	-7.42	-7.67	-7.97	-11.24
P3	-2.40	-3.04	-4.33	-7.08	-7.62	-7.82	-8.19	-11.20
P3+	-2.32	-2.92	-3.99	-6.89	-7.40	-7.63	-7.93	-10.96
Expt. ^(a)	2.145±0.01							

^a Experimental value = 2.145 ± 0.01 eV. *This state has pole strengths near 0.80 for all approximations beyond KT. ^(a) Experimental value from ref 10.

TABLE 4: Vertical Electron Detachment Energies (eV) and Orbitals for Diazolides^a

	² A ₂ ⁺	² B ₁	² B ₂	² A ₁	² B ₂	² B ₁
KT	-3.26	-3.40	-5.38	-6.87	-9.36	-9.51
2Ord	-2.80	-2.86	-2.49	-3.94	-7.24	-6.94 *
3Ord	-3.40	-3.42	-4.76	-6.27	-8.45	-8.49 *
OVSF	-3.22	-3.12	-3.80	-5.29	-7.91	-7.87 *
P3	-3.41	-3.44	-3.99	-5.47	-8.14	-7.84
P3+	-3.29	-3.33	-3.63	-5.09	-7.95	-7.62

	² B ₁ (⁺)	² A ₂	² B ₂	² A ₁	² A ₁	² B ₁
KT	-2.63	-4.20	-5.83	-6.83	-9.37	-9.56
2Ord	-2.46	-3.23	-2.97	-4.18	-7.26	-7.10 *
3Ord	-2.83	-4.12	-5.13	-6.12	-8.60	-8.56 *
OVSF	-2.73	-3.72	-4.25	-5.32	-8.03	-7.98 *
P3	-2.92	-4.00	-4.40	-5.48	-8.21	-7.96 *
P3+	-2.84	-3.85	-4.07	-5.19	-8.01	-7.76 *

^a Experimental value = 2.938 ± 0.005 eV. Experimental value = 2.613 ± 0.006 eV. *Pole strengths are between 0.79 and 0.84.




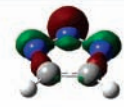



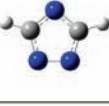
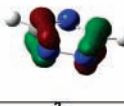
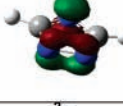

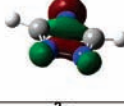
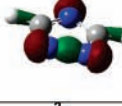
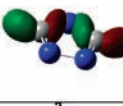
centered π orbital pertains to the next final state. Antibonding and bonding combinations of nitrogen lone-pair orbitals are bound more strongly than the π orbitals, with the in-phase nitrogen lone-pair combination being the more tightly held. Because of the stabilizing role of the nitrogen atoms, the orbitals centered on them are more stable compared to those that are primarily centered on the carbon atoms. Lone-pair orbitals correspond to higher VEDEs than the π orbital combinations involving nitrogens. The magnitude of correlation corrections is also much larger for orbitals mainly made of the nitrogen lone-pairs lobes than for the nitrogen or carbon-based π orbitals.

The pyrrolide anion has nitrogen atoms in proximity to each other, which facilitates localization on nitrogen atoms and the strengthening of the binding energies of all orbitals. The proximity of the two nitrogens reverses the energy ordering and centering of orbitals in these two isomers. The b_1 C–C π orbital of the imidazolide is replaced by a predominantly N–N π orbital of the same symmetry which is more bound due to proximity of the participating N atoms. There is a similar reversal in the character of the a_2 HOMO-1 orbital of the imidazolide, which becomes the HOMO of this isomer. A larger contribution from

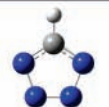

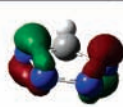
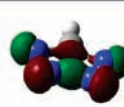

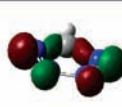
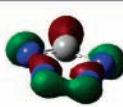
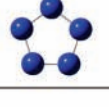
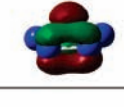
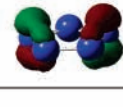
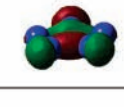
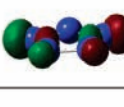
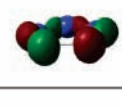
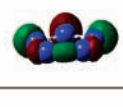
carbon atoms moves this orbital to a lower VEDE. Other features for the pyrrolide are broadly similar to those discussed for imidazolide, and the orbitals which display bonding and antibonding combinations of the nitrogen lone pairs again lie deeper than the π orbital that involves larger participation of carbon atoms in the ring. The correlation corrections to KT results for these predominantly nitrogen lone-pair-based orbitals are significantly larger than those for the π orbitals. There is a reordering of the deeper b_2 and b_1 orbitals in this system when correlation corrections are incorporated.

Triazolides. The first electron detachment energies for the 1,2,3- and 1,2,4-triazolide anions are larger than those of the diazoles. There is a reversal of the order of the ²A₂ and ²B₁ final states between the two isomers. For the a_2 Dyson orbitals, there is a symmetry-imposed nodal plane, perpendicular to the nuclear plane, that passes through the atom that lies on the C₂ axis and that lies between π orbital lobes that span the C–N bonds. These lobes have higher amplitudes near the more electronegative nitrogens. The antibonding effect of the node is greater when the two nitrogens are neighbors than when they are separated by the third nitrogen. Therefore, the a_2 electron

TABLE 5: Vertical Electron Detachment Energies (eV) and Orbitals for Triazolides^a

						
<i>KT</i>	² B ₁	² A ₂	² A ₁	² B ₂	² A ₁	² B ₁
<i>2Ord</i>	-3.70	-4.53	-6.11	-6.17	-8.08	-10.42
<i>3Ord</i>	-3.39	-3.84	-3.34	-3.34	-5.25 *	-7.74 *
<i>3Ord</i>	-3.79	-4.51	-5.39	-5.42	-7.22	-9.32 *
<i>OVGF</i>	-3.67	-4.15	-4.46	-4.50	-6.35	-8.66 *
<i>P3</i>	-3.91	-4.53	-4.80	-4.81	-6.61	-8.68 *
<i>P3+</i>	-3.82	-4.40	-4.45	-4.47	-6.29	-8.45 *
						
<i>KT</i>	² A ₂	² B ₁	² B ₂	² A ₁	² A ₁	² B ₂
<i>2Ord</i>	-3.68	-4.82	-6.07	-6.39	-8.24	-10.05
<i>2Ord</i>	-3.34	-3.86	-3.21	-3.58	-5.66 *	-8.02
<i>3Ord</i>	-3.84	-4.69	-5.38	-5.66	-7.68	-9.26
<i>OVGF</i>	-3.69	-4.30	-4.48	-4.80	-6.83	-8.71
<i>P3</i>	-3.90	-4.61	-4.64	-4.98	-7.02	-8.95
<i>P3+</i>	-3.80	-4.47	-4.31	-4.66	-6.70	-8.76

^a Pole strength is near 0.80.TABLE 6: Vertical Electron Detachment Energies (eV) and Orbitals for Tetrazolide and Pentazolide^a

						
<i>KT</i>	² B ₁	² A ₂	² A ₁	² B ₂	² B ₂	² A ₁
<i>2Ord</i>	-4.67	-5.41	-6.69	-6.84	-7.13	-9.79
<i>2Ord</i>	-4.34	-4.65	-3.96 *	-4.11 *	-4.40 *	-7.14 *
<i>3Ord</i>	-4.74	-5.30	-5.87	-6.06	-6.34	-9.03
<i>OVGF</i>	-4.62	-4.93	-4.98	-5.16	-5.48	-8.17
<i>P3</i>	-4.91	-5.35	-5.37	-5.54	-5.78	-8.47
<i>P3+</i>	-4.81	-5.22	-5.04	-5.20	-5.46	-8.15
						
<i>KT</i>	² E ₁ ''	² E ₁ '	² E ₂ '	² E ₂ '	² E ₂ '	² E ₂ '
<i>2Ord</i>	-5.97	-7.43	-7.98	-7.98	-7.98	-7.98
<i>2Ord</i>	-5.49	-4.71	-5.44	-5.44	-5.44	-5.44
<i>3Ord</i>	-5.89	-6.55	-7.20	-7.20	-7.20	-7.20
<i>OVGF</i>	-5.76	-5.66	-6.34	-6.34	-6.34	-6.34
<i>P3</i>	-6.12	-6.12	-6.80	-6.80	-6.80	-6.80
<i>P3+</i>	-6.00	-5.79	-6.48	-6.48	-6.48	-6.48

^a Pole strength is near 0.84.

detachment energy for the 1,2,4 isomer is lower. Dyson orbitals for the ²B₁ final states also display nodal surfaces that are perpendicular to the nuclear plane. Instead of imposing low amplitudes on one, symmetry-unique atom, as in the a₂ case, these b₁ orbitals minimize amplitudes on the two neighboring atoms. Opposite phases obtain on the two-center and one-center lobes that are separated by this nodal plane. A higher electron binding energy is associated with the 1,2,4 isomer in which the two-center lobe spans a bond between two N atoms. Therefore, a lower electron detachment energy results for the b₁ Dyson orbital of the 1,2,3 isomer. For the next two electron detachment energies, there is another reversal of the order of states. In the

b₂ Dyson orbitals, there is an out-of-phase combination of lone-pair lobes on the two symmetry-equivalent N atoms. This antibonding relationship is more powerful when the two N atoms are neighbors and the associated electron detachment energy is somewhat lower for the 1,2,4 isomer. (Note that the P3+ result changes the order of the ²B₁ and ²B₂ final states.) Out-of-phase relationships are seen in the a₁ Dyson orbitals between the central N atom's lone-pair lobe and those of the other two N atoms. When the three N atoms are adjacent, this antibonding effect grows more important, and the associated electron binding energy is less than its 1,2,4 counterpart where carbon atoms lie between nitrogens. For both isomers, the fifth electron detach-

ment energy corresponds to an a_1 Dyson orbital with N-centered nonbonding and C–H bonding lobes. Reasonably large pole strengths accompany the sixth electron detachment energy of one isomer, but the validity of the present electron propagator decouplings for the other isomer's sixth final state is questionable.

The pattern seen for the diazoles repeats itself: larger N orbital contributions are associated with larger binding energies. The correlation corrections are once again substantially larger for the orbitals made up from the N lone-pair lobes than for the π orbitals. The second-order approximation tends to overestimate the effects of relaxation and correlation. Higher order corrections remain important for determining the correct order of final states.

Tetrazolide and Pentazolide. Carbon contributions to the b_1 Dyson orbital lead to a lower electron binding energy for the 2B_1 final state than for the 2A_2 final state. The nodal pattern seen for the triazolide b_1 Dyson orbitals is repeated in the tetrazolide. Larger amplitudes on the 2 and 5 N atoms reduce antibonding interactions across the N_3 – N_4 bond in the a_2 Dyson orbital. Lone-pair lobes are more prominent on the N_3 and N_4 atoms in the following a_1 and b_2 Dyson orbitals. The next two σ orbitals are more concentrated on the N_2 and N_5 positions. OVGf, P3 and P3+ results for the second through the fifth final states are within 0.5 eV of each other. C–H bonding contributions are important only in the Dyson orbital for the last 2A_1 final state.

The highest electron detachment energies are found for the pentazolide. Degenerate pairs of Dyson orbitals follow from the D_{5h} point group of this anion. The e_1'' π orbital set is followed by the e_1' and e_2' sets at the uncorrelated level, but the order is changed in OVGf, P3, and P3+ calculations. The net effect of correlation and relaxation for the π holes is relatively small and leads to slightly increased electron detachment energies. Large decreases arise from correlated calculations on σ holes.

Splittings between the pairs of tetrazolide final states that resemble their doubly degenerate counterparts in the pentazolide are much larger for the fifth 2B_2 and sixth 2A_1 cases. In the latter case, there is a lobe that corresponds to C–H σ bonding that may be responsible for the much lower energy of the corresponding Dyson orbital.

IV. Conclusions

A uniform treatment of the electron detachment energies of an important family of anions, the azolides, has been generated with ab initio electron propagator calculations. Close agreement with experiment obtains for the lowest VEDEs of pyrrolide and imidazolide with the OVGf, P3, and P3+ approximations. These results and calculations on other electron binding energies reveal the importance of electron correlation in making accurate predictions, including the correct order of final states. Correlation and relaxation corrections to Koopmans results are larger for final states with σ holes versus those with π holes. VEDEs increase with the substitution of N atoms for CH groups. Reorderings of final states between isomers may be based on

phase relationships and the positions of nodal surfaces. Radical doublets with π holes are lower in energy than those with σ holes in all cases except N_5^- . Many higher VEDEs lie within the reach of photon sources which are currently available to practitioners of anion photoelectron spectroscopy. Additional refinements to the present predictions await the report of such experiments.

Acknowledgment. The National Science Foundation provided support through grants CHE-0135823 and CHE-0451810 to Kansas State University. M.K.M. is pleased to acknowledge support from DST grant SP/S1/H-18/2001 to IIT Bombay.

References and Notes

- (1) Fau, S.; Wilson, K. J.; Bartlett, R. J. *J. Phys. Chem. A* **2002**, *106*, 4639.
- (2) Gagliardi, L.; Orlandi, G.; Evangelisti, S.; Roos, B. O. *J. Chem. Phys.* **2001**, *114*, 10733.
- (3) Nguyen, M. T.; Ha, T. K. *Chem. Phys. Lett.* **2001**, *335*, 311.
- (4) Vianello, R.; Maksic, Z. B. *Mol. Phys.* **2005**, *103*, 209.
- (5) Vij, A.; Wilson, W. W.; Vij, V.; Tham, F. S.; Sheehy, J. A.; Christe, K. O. *J. Am. Chem. Soc.* **2001**, *123*, 6308.
- (6) Vij, A.; Pavlovich, J. G.; Wilson, W. W.; Vij, V.; Christe, K. O. *Angew. Chem. Int. Ed.* **2002**, *41*, 3051.
- (7) Butler, R. N.; Stephens, J. C.; Burke, L. A. *Chem. Commun.* **2003**, 1016.
- (8) Ostrovskii, V. A.; Brusilimskii, G. B.; Shcherbinin, M. B. *Z. Org. Khimi* **1995**, *31*, 1422.
- (9) Gianola, A. J.; Ichino, T.; Hoeningman, R. L.; Kato, S.; Bierbaum, V. M.; Lineberger, W. C. *J. Phys. Chem. A* **2004**, *108*, 10326.
- (10) Gianola, A. J.; Ichino, T.; Hoeningman, R. L.; Kato, S.; Bierbaum, V. M.; Lineberger, W. C. *J. Phys. Chem. A* **2005**, *109*, 11504.
- (11) Gianola, A. J.; Ichino, T.; Kato, S.; Bierbaum, V. M.; Lineberger, W. C. *J. Phys. Chem. A* **2006**, *110*, 8457.
- (12) Kurup, A.; Garg, R.; Carini, D. J.; Hansch, C. *Chem. Rev.* **2001**, *101*, 2727.
- (13) Linderberg, J.; Öhrn, Y. *Propagators in Quantum Chemistry*, 2nd ed.; Wiley: Hoboken, NJ, 2004.
- (14) Ortiz, J. V. *Adv. Quantum Chem.* **1999**, *33*, 35.
- (15) Mishra, M. K.; Medikeri, M. N. *Adv. Quantum Chem.* **1996**, *27*, 225.
- (16) (a) Ferreira, A. M.; Seabra, G.; Dolgounitcheva, O.; Zakrzewski, V. G.; Ortiz, J. V. In *Quantum Mechanical Predictions of Thermochemistry Data*; Cioslowski, J., Ed.; Kluwer: Dordrecht, 2001; p 131. (b) Ortiz, J. V. In *Computational Chemistry: Reviews of Quantum Current Trends*; Leszczynski, J., Ed.; World Scientific: Singapore, 1997; Vol. 2, p 1. (c) Venkatnathan, A.; Mahalakshmi, S.; Mishra, M. K. *J. Chem. Phys.* **2001**, *114*, 35. (d) Mahalakshmi, S.; Venkatnathan, A.; Mishra, M. K. *J. Chem. Phys.* **2001**, *115*, 4549.
- (17) *Gaussian03, Revision B.03*; Frisch, M. J.; Trucks, G. W.; Schlegel, H.; Scuseria, G. E.; Robb, M. A.; Cheeseman, J. R.; Montgomery, J. A., Jr.; Vreven, T.; Kudin, K. N.; Burant, J. C.; Millam, J. M.; Iyengar, S. S.; Tomasi, J.; Barone, V.; Mennucci, B.; Cossi, M.; Scalmani, G.; Rega, N.; Petersson, G. A.; Nakatsuji, H.; Hada, M.; Ehara, M.; Toyota, K.; Fukuda, R.; Hasegawa, J.; Ishida, M.; Nakajima, T.; Honda, Y.; Kitao, O.; Nakai, H.; Klene, M.; Li, X.; Knox, J. E.; Hratchian, H. P.; Cross, J. B.; Adamo, C.; Jaramillo, J.; Gomperts, R.; Stratmann, R. E.; Yazyev, O.; Austin, A. J.; Cammi, R.; Pomelli, C.; Ochterski, J. W.; Ayala, P. Y.; Morokuma, K.; Voth, G. A.; Salvador, P.; Dannenberg, J. J.; Zakrzewski, V. G.; Dapprich, S.; Daniels, A. D.; Strain, M. C.; Farkas, O.; Malick, D. K.; Rabuck, A. D.; Raghavachari, K.; Foresman, J. B.; Ortiz, J. V.; Cui, Q.; Baboul, A. G.; Clifford, S.; Cioslowski, J.; Stefanov, B. B.; Liu, G.; Liashenko, A.; Piskorz, P.; Komaromi, I.; Martin, R. L.; Fox, D. J.; Keith, T.; Al-Laham, M. A.; Peng, C. Y.; Nanayakkara, A.; Challacombe, M.; Gill, P. M. W.; Johnson, B.; Chen, W.; Wong, M. W.; Gonzalez, C.; Pople, J. A. *Gaussian, Inc.*: Pittsburgh, PA, 2003.
- (18) Ortiz, J. V. *Int. J. Quantum Chem.* **2005**, *105*, 803.